Untangling the effects of peptide sequences and nanotopographies in a biomimetic niche for directed differentiation of iPSCs by assemblies of genetically engineered viral nanofibers

Jianglin Wang[†&], Lin Wang[†&], Mingying Yang[‡†&], Ye Zhu[†], Antoni Tomsia[§] and Chuanbin Mao*[†]*

†Department of Chemistry and Biochemistry, Stephenson Life Sciences Research Center, University of Oklahoma, Norman, OK 73019, USA

‡Institute of Applied Bioresource Research, College of Animal Science, Zhejiang University, Yuhangtang Road 866, Hangzhou, Zhejiang 310058, China

§Materials Science Division, Lawrence Berkeley National Laboratory, One Cyclotron Road Berkeley, CA 94720, USA

Corresponding authors:

Mingying Yang, E-mail: yangm@zju.edu.cn, Fax: +86-571-88982185

Chuanbin Mao, E-mail: cbmao@ou.edu, Fax: +1-405-325-6111

Supplementary Information (SI):

Materials and Methods

Peptide display and phage-assembled matrix. Four peptides (Figure 1E) were displayed on the N-terminus of pVIII, which was the major coat protein constituting the external side wall of M13 bacteriophage, by following our reported protocols.[1, 2] All bioengineered phages were used to prepare phage-assembled matrix with ordered surface nanotopography at a constant phage concentration of 10^{14} pfu/ml using a layer-by-layer self-assembly method established by our group[2] (Figure 2A). The corresponding phage matrix with random surface nanotopography as a random control was also fabricated through a spinning-drying method (Figure S2). The poly-lysine substrate without phage matrix was designed as a blank control.

Mouse iPSCs culture and EB formation. The mouse iPSCs were commercially purchased (Applied Stem cell Inc, CA) and maintained on the feeder layers of mitomycin C-treated mouse embryonic fibroblast (MEF) as previously described.[3] The iPSCs were expanded in the embryonic stem cell (ESC) medium containing KNOCKOUT^{TM} DMEM, 10% ESC qualified fetal bovine serum (ESC-FBS, Gibco), 1000 U/ml leukemia inhibitory factor (LIF), 2 mM Glutamax-I, 0.1 mM non-essential amino acid (NEAA), 0.1 mM β-mercaptoethanol, 50 U/ml penicillin, and 50 μg/ml streptomycin. Embryonic bodies (EBs) were derived from iPSCs by a reported hanging-drop method and cultured in the above EB medium devoid of LIF.[4]

Cell seeding and culture on phage-assembled matrix. The EBs were seeded on phage matrix and co-cultured in a mesenchymal differentiation medium including KNOCKOUT^{TM} DMEM, 10% ESC-FBS, 10^{-7} M all-trans retinoic acid (RA), 2 mM Glutamax-I, 0.1 mM non-essential amino acid, 0.1 mM β-mercaptoethanol, 50 U/ml penicillin, and 50 μg/ml streptomycin [3]. After EBs were cultured for 3 days, the mesenchymal differentiation medium was switched to EB medium, and the medium was changed every 2-3 days. Upon reaching confluence, cells were trypsinized and subcultured on phage matrix with EB medium for 2 weeks until all cells turned into fibroblast-like cells. For osteoblastic differentiation study, the basal medium (low glucose DMEM supplemented with 10% MSCs-FBS) without any osteogenic supplements was used to culture these fibroblast-like cells for 2 weeks. The phenotype analysis and morphological change of resident EBs onto phage matrix were investigated during the differentiation process.

Phenotype analysis of mesenchymal progenitor cells from iPSC-derived EBs. After co-cultured for 3 days on the phage matrix, the induced EBs were collected for analyzing surface antigens of mesenchymal markers by flow cytometry and immunofluorescence staining.

Evaluation of osteogenic differentiation. The ALP activity was first used to verify the osteoprogenitor and performed by the p-nitrophenyl phosphate (pNPP) method [2]. Immunofluorescence staining was used to evaluate the osteo-specific markers at the protein level. The cells on phage matrix were washed with PBS and fixed with 4% paraformaldehyde at 4°C for 30 min, permeablized using 0.3% Triton X-100 for 5 min, and then blocked with 5% goat serum solution for 1 h at room temperature. After blocking, the cells were incubated overnight at 4°C with the primary antibodies targeting the osteo-specific proteins (Osteocalcin [OCN] and osteopontin [OPN]) and non-osteo-specific protein (collagen I-α1, COL). Secondary antibody conjugated with Rhodamine was used for labeling OCN, OPN, and COL, respectively,

at 1:1000 dilutions in a blocking buffer for 1 h at room temperature. FITC-labeled phallodin (1:400 in PBS) and DAPI (4,6-diamidino-2-phenylindole) were used to stain the actin filaments and nuclei, respectively. Real-time PCR was further assayed by Ambion Power SYBR Green Cells-to-Ct Kit (Invitrogen, US). The template cDNA was amplified with real-time quantitative PCR using gene-specific primers of OCN, OPN, and COL. Acidic ribosomal phosphoprotein (Arbp) was used as a reference gene. Sequences of the primers in this study were used based on our recent publication. [2]

Teratoma formation in vivo. To estimate the clinical potential of iPSCs-derived osteoblasts (iPSCs-OBs), we analyzed their teratoma formation in vivo. Both iPSCs-OBs and pure iPSCs were injected subcutaneously into the back of Athymic Nude-Foxn1nu mice (5 week old, female, Harlan). The animals were monitored for 1 month for teratoma formation, and the generated teratoma was removed for further histological analysis. The teratoma were firstly fixed in a 10% neutral formalin solution, and subsequently embedded in paraffin by a Paraffin Embedder (Leica EG 1160). They were then sectioned into slices of a thickness of around 5 μm using a Paraffin Microtome (Leica RM 2155) and stained with hematoxylin and eosin to verify the differentiation potential of three layers of germ cell.

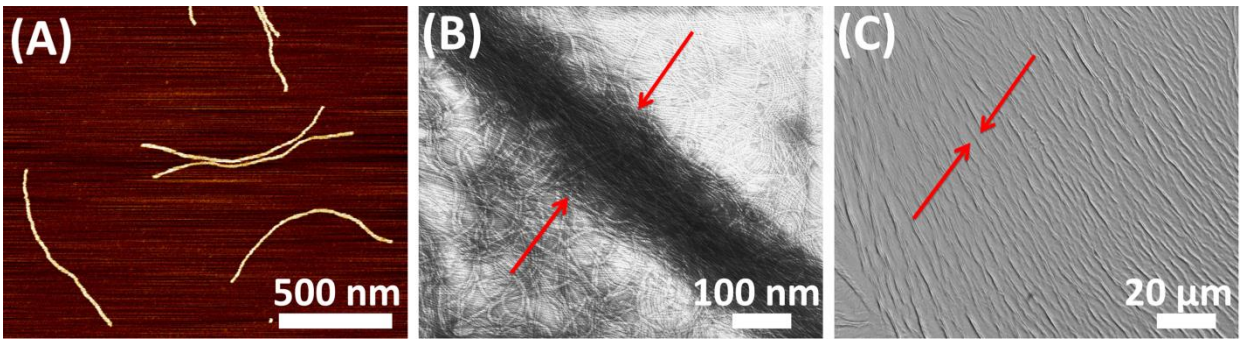

Figure S1. Gradual assembly of phage bionanofibers from the bottom up. (A) AFM image shows the morphology of individual phage with ~880 nm in length and ~6.6 nm in width. (B) TEM image shows phage bundle assembled from individual phage nanofibers. (C) Optical image shows phage matrix assembled by phage bundles. Red arrows are used to highlight the width of the phage bundles.

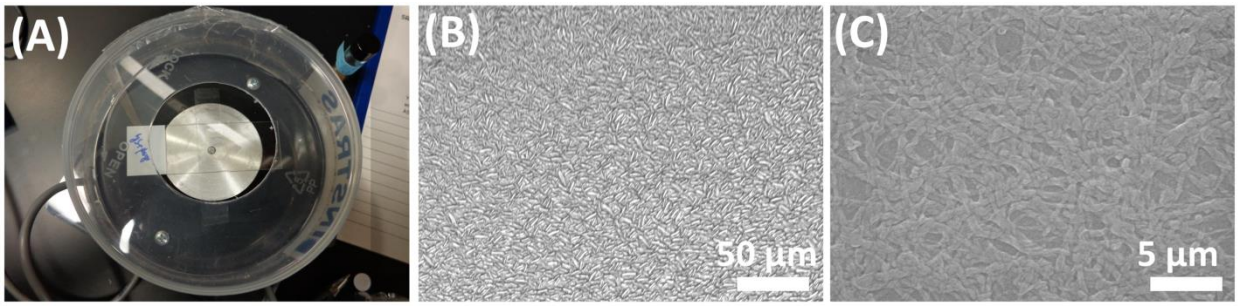

Figure S2. Fabrication and characterization of phage matrix with random nanotopography. The phage-assembled matrix with random surface nanotopography as a control for phage matrix with ordered nanotopography was fabricated by a spinning-drying method (A). The resultant phage matrix shows a random distribution (B, optical image; C, SEM image)

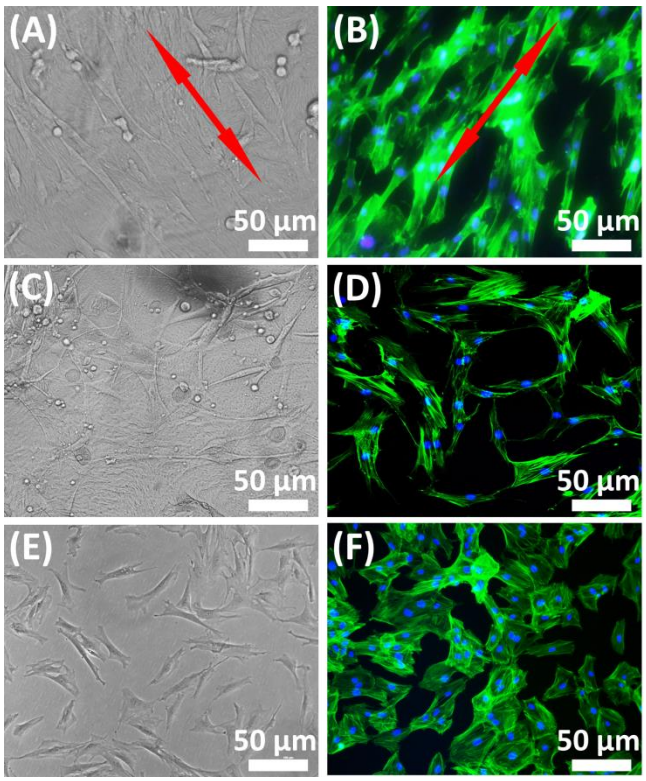

Figure S3. Morphological difference of iPSCs-derived MPCs on ordered, random and smooth substrates. The resident cells show an oriented alignment with significant elongation on the phage matrix with an ordered nanotopography (A, optical image; B, fluorescent image). The resident cells are randomly oriented on the phage matrix with a random nanotopography (C, optical image; D, fluorescent image). The resident cells are also randomly oriented on the smooth substrate (poly-lysine substrate without any phage matrix). The red arrows in A and B denote the direction of cell elongation. Cell nuclei were stained by DAPI (blue) and F-actin were stained by FITC-labeled phalloidin (green).

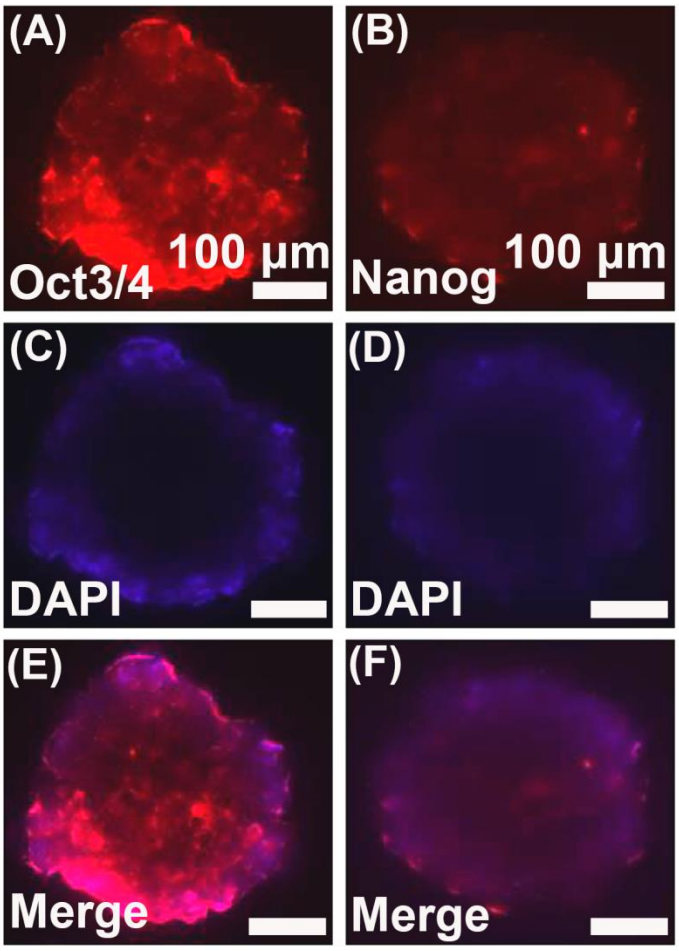

Figure S4. Characterization of embryonic body (EB). The specific pluripotent markers of Oct3/4 and Nanog show positive staining, presenting a classic rosette staining (E, F). (A and B, positive staining of Oct3/4 and Nanog; C and D, nucleus staining with DAPI; E and F, merged images).

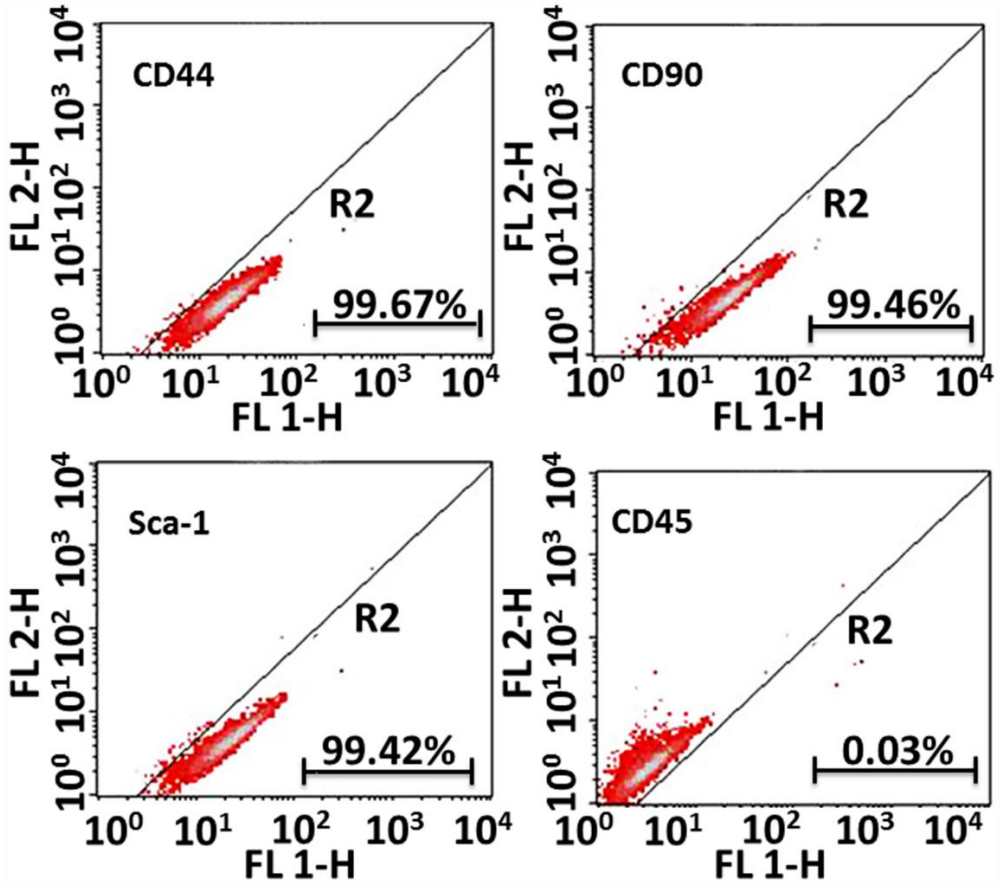

Figure S5. Flow cytometry for quantifying surface antigens of rat MSCs. CD44, CD90, and Sca-1 show positive expression whereas CD45 served as a negative marker in rat MSCs.

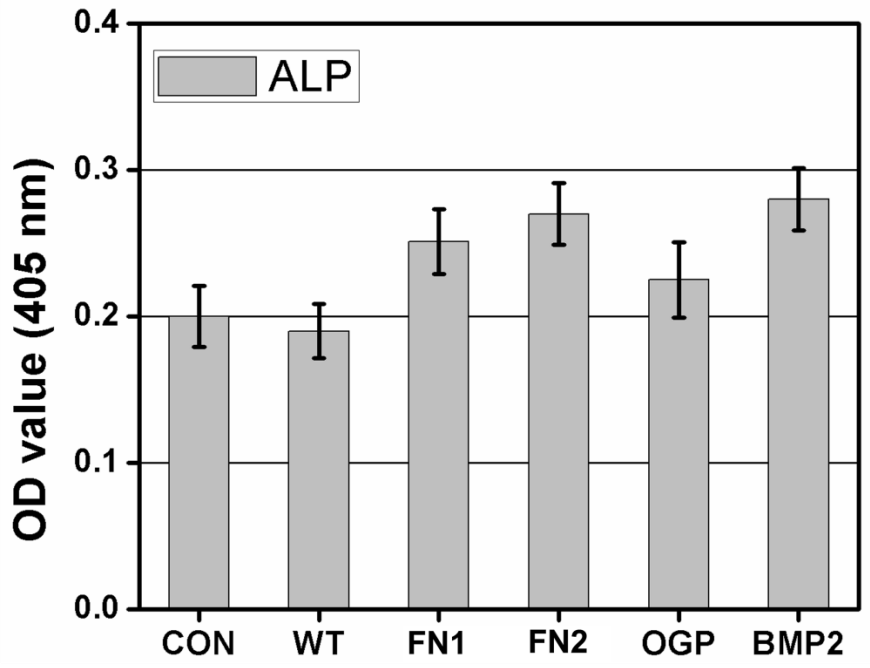

Figure S6. ALP analysis for the phage matrix with a random nanotopography. There is no significant difference between the phage matrix and control. CON denotes control (poly-L-lysine substrates without phage). WT, FN1, FN2, OGP and BMP2 denotes the phage matrix made of WT-phage, FN1-phage, FN2-phage, OGP-phage and BMP2-phage, respectively.

References:

(1) Zhu, H.; Cao, B.; Zhen, Z.; Laxmi, A. A.; Li, D.; Liu, S.; Mao, C. *Biomaterials* **2011,** 32, 4744-4752.
(2) Wang, J.; Wang, L.; Li, X.; Mao, C. *Sci. Rep.* **2013,** 3, 1242.
(3) Bilousova, G.; Jun, D. H.; King, K. B.; De Langhe, S.; Chick, W. S.; Torchia, E. C.; Chow, K. S.; Klemm, D. J.; Roop, D. R.; Majka, S. M. *Stem Cells* **2011,** 29, 206-216.
(4) Takahashi, K.; Yamanaka, S. *Cell* **2006,** 126, 663-676.